Since January 2020 Elsevier has created a COVID-19 resource centre with free information in English and Mandarin on the novel coronavirus COVID-19. The COVID-19 resource centre is hosted on Elsevier Connect, the company's public news and information website.

Elsevier hereby grants permission to make all its COVID-19-related research that is available on the COVID-19 resource centre - including this research content - immediately available in PubMed Central and other publicly funded repositories, such as the WHO COVID database with rights for unrestricted research re-use and analyses in any form or by any means with acknowledgement of the original source. These permissions are granted for free by Elsevier for as long as the COVID-19 resource centre remains active.

Biosensors and Bioelectronics 217 (2022) 114710

Contents lists available at ScienceDirect

Biosensors and Bioelectronics

journal homepage: www.elsevier.com/locate/bios

Ultrasensitive monitoring of SARS-CoV-2-specific antibody responses based on a digital approach reveals one week of IgG seroconversion

Feiyang Ou [a,1], Danyun Lai [b,1], Xiaojun Kuang [a], Ping He [c,d], Yang Li [b], He-wei Jiang [b], Wei Liu [e], Hongping Wei [c], Hongchen Gu [a], Yuan qiao Ji [f], Hong Xu [a,*], Sheng-ce Tao [b,**]

[a] School of Biomedical Engineering, Med-X Research Institute, Shanghai Jiao Tong University, Shanghai, 200030, China
[b] Shanghai Center for Systems Biomedicine, Shanghai Jiao Tong University, Shanghai, 200240, China
[c] CAS Key Laboratory of Special Pathogens and Biosafety, Centre for Biosafety Mega-Science, Wuhan Institute of Virology, Chinese Academy of Sciences, Wuhan, Hubei, 430071, China
[d] University of Chinese Academy of Sciences, Beijing, 100049, China
[e] Hangzhou Joinstar Biotechnology Co., Ltd. Hangzhou, 310000, China
[f] YK Pao School, Shanghai, 201620, China

ARTICLE INFO

Keywords:
COVID-19
Ultrasensitive digital detection
Extreme early-stage seroconversion
IgG/IgM antibodies
Diagnostic

ABSTRACT

COVID-19 is still unfolding, while many people have been vaccinated. In comparison to nucleic acid testing (NAT), antibody-based immunoassays are faster and more convenient. However, its application has been hampered by its lower sensitivity and the existing fact that by traditional immunoassays, the measurable seroconversion time of pathogen-specific antibodies, such as IgM or IgG, lags far behind that of nucleic acids. Herein, by combining the single molecule array platform (Simoa), RBD, and a previously identified SARS-CoV-2 S2 protein derivatized 12-aa peptide (S2-78), we developed and optimized an ultrasensitive assay (UIM-COVID-19 assay). Sera collected from three sources were tested, *i.e.*, convalescents, inactivated virus vaccine-immunized donors and wild-type authentic SARS-CoV-2-infected rhesus monkeys. The sensitivities of UIM-COVID-19 assays are 100–10,000 times higher than those of conventional flow cytometry, which is a relatively sensitive detection method at present. For the established UIM-COVID-19 assay using RBD as a probe, the IgG and IgM seroconversion times after vaccination were 7.5 and 8.6 days *vs.* 21.4 and 24 days for the flow cytometry assay, respectively. In addition, using S2-78 as a probe, the UIM-COVID-19 assay could differentiate COVID-19 patients (convalescents) from healthy people and patients with other diseases, with AUCs ranging from 0.85–0.95. In summary, the UIM-COVID-19 we developed here is a promising ultrasensitive biodetection strategy that has the potential to be applied for both immunological studies and diagnostics.

1. Introduction

COVID-19, caused by SARS-CoV-2, has aroused a huge global impact. As of April 17, 2022, there have been 504 million infected people around the world (https://coronavirus.jhu.edu/map.html)(Dong et al., 2020). Accurate and early diagnosis is a key step to control the pandemic. Although nucleic acid testing (NAT) is the gold standard in detecting SARS-CoV-2 infection, serological testing is an essential complement to NAT, especially for fast detection and the monitoring of mild or asymptomatic infections (Lee et al., 2020). In addition, because of the high correlation between SARS-CoV-2-specific antibody responses against RBD and serum neutralization activity (Ma et al., 2021), serological testing is the most convenient way to estimate the serum neutralization activity for both COVID-19 patients and vaccinated people (Xue et al., 2022). More importantly, IgM and IgG play critical roles during infection and recovery; for example, the SARS-CoV-2-specific IgG response can be used as an index of infection and previous infection (Woo et al., 2004). It is generally believed that SARS-CoV-2-specific IgM antibodies will appear within 7 days after infection for a rapid and urgent immune reaction (Bosnjak et al., 2021), while SARS-CoV-2-specific IgG antibodies will appear after 14 days. These time windows for seroconversion are also widely recognized for many other viral infections

* Corresponding author.
** Corresponding author.
E-mail addresses: xuhong@sjtu.edu.cn (H. Xu), taosc@sjtu.edu.cn (S.-c. Tao).
[1] These authors contributed equally to this work.

https://doi.org/10.1016/j.bios.2022.114710
Received 18 May 2022; Received in revised form 11 August 2022; Accepted 6 September 2022
Available online 15 September 2022
0956-5663/© 2022 Elsevier B.V. All rights reserved.

(Gaylord et al., 2015; Xie et al., 2022). Because of this, the common knowledge is that serological testing is not suitable for the early detection or monitoring of COVID-19 and other infections and limits its clinical application. The most traditional method for serological testing is enzyme-linked immunosorbent assay (ELISA), usually with a pg/mL ultimate sensitivity. However, we believe that the appearance of SARS-CoV-2-specific antibodies after infection or vaccination is gradually progressing. Thus, we hypothesize that the seroconversion times for both IgG and IgM could be reliably shortened if a method with much higher sensitivity than ELISA is applicable. By then, we can detect COVID-19 by immunoassay at a much earlier time point, which will promote the antibody detection assay to play a more essential role in practical clinical diagnosis.

Single molecule array (Simoa), has shown unique advantages in clinical applications, especially in the detection of low abundance proteins or biomarkers due to its high sensitivity (Preische et al., 2019). Compared with traditional ELISA tests, Simoa has also played a great role in the detection of antigens and antibodies (Cai et al., 2021; Norman et al., 2020; Shan et al., 2021), neutralizing antibodies (Gilboa et al., 2021) and vaccine monitoring (Ogata et al., 2021) in body fluids during the COVID-19 pandemic, contributing greatly to the in-depth understanding of COVID-19 and the development of new detection and monitoring methods. However, most of the current seroconversion studies start from the onset of symptoms, while the number of days of infection before the onset of symptoms is unknown. In addition, the human challenge trial (Killingley et al., 2022) and animal model tests (Ryan et al., 2021) could also not provide precise time of earlier seroconversion; thus, the early seroconversion surveillance of IgG and IgM antibodies was not achieved.

Additionally, for antibody detection aimed at SARS-CoV-2, in addition to using traditional antigens as probes, *i.e.*, the N protein and S protein, another widely applied antigen is RBD. The reason is that the overall performance of RBD is similar to that of N protein and S protein, but the antibody response to RBD is related to serum neutralization activity (Brouwer et al., 2020). In addition, according to our previous study, a SARS-CoV-2 spike protein-derived peptide, S2-78 (aa 1148–1159), can be applied to detect asymptomatic infections (Li et al., 2021a; Speer et al., 2021), and the overall diagnostic performance of S2-78 is comparable to that of the S protein. Importantly, there are several advantages of peptide-based detection when compared to protein or protein domain-based detection. For example, higher stability, lower cost, and ease of scaling up in a very short period by chemical synthesis, *etc*.

Herein, we combined RBD/S2-78 peptide and the single molecule detection power of Simoa and developed an ultrasensitive immunoassay. This assay was applied to monitor the SARS-CoV-2-specific antibody responses induced by an inactivated virus vaccine or SARS-CoV-2 infection. Highly sensitive detection was achieved, and it is exciting to find that the seroconversion time revealed by this assay is approximately two weeks earlier than by flow cytometry, which improves our understanding of the seroconversion time window after virus infection.

2. Materials and methods

2.1. Sample collection and cohorts

Eight vaccination participants were enrolled in this study. The participants were immunized with the inactivated virus vaccine, and serum samples were collected at 10 time points after the 1st dose and 2nd dose (Cohort 1 in Table 1). Sera from 47 COVID-19 convalescent patients, 43 healthy controls and 50 other diseases, including lung cancer and non-respiratory diseases, were collected from Foshan Fourth Hospital, Foshan, Tongren Hospital, Shanghai and Ruijin Hospital, Shanghai. The serum samples were collected on the day of hospital discharge (Cohort 2, Cohort 3 and Cohort 4 in Table 1). The rhesus monkey sera were provided by Wuhan Institute of Virology, Wuhan, China. Two rhesus monkeys were infected with the reference strain of SARS-CoV-2, and the other two were infected with the B.1.351 variant (Cohort 5 in Table 1). Samples were taken for 8 consecutive days from the beginning of the infection. All the samples were strictly inactivated (56 °C water bath for 30 min). All samples were stored at −80 °C until use.

Ethical approval

The study was approved by the Institutional Ethics Review Committee of Foshan Fourth Hospital, Foshan, China (ref. no. 202005), and the Ethics Commission of Shanghai Jiao Tong University (ref. no. B2021120I). Written informed consent was obtained from each participant. The infected rhesus sera collection was approved by Wuhan Institute of Virology (WIVA42202006; WIVA42202002-01).

2.2. S2-78 peptides conjugated on magnetic microbeads

The S2-78 peptides, belonging to the spike protein of SARS-CoV-2 (aa 1148–1159) and containing 12 amino acids (FKEELDKYFKNH), were synthesized by GL Biochem, Ltd. (Shanghai, China). To conjugate S2-78 peptides onto the magnetic beads, the peptide was modified with a cysteine. Briefly, the magnetic beads were modified with PEI (Sigma–Aldrich, Missouri, USA, Cat No. 181978-250G) to endow the amino groups onto the surface of beads. Then, 400 μL of 4 mg/mL Sulfo-SMCC (Sigma–Aldrich, Missouri, USA, Cat No. M6035) was mixed with 1 mg PEI-modified beads in a 2 mL centrifuge tube and incubated at 25 °C for 1 h. After washing three times, 400 μL of 0.1 mg/mL S2-78 peptide PBS solution was added and incubated at 25 °C for 2 h. The S2-78 beads were washed three times with PBST (10 mM, pH = 7.4) and stored in 100 μL PBST for subsequent use.

Table 1
Samples used in this study.

		Cohort 1	Cohort 2	Cohort 3	Cohort 4	Cohort 5
Group		Vaccination	Convalescent	Healthy control	Other diseases	Infected rhesus
Numbers		8	47	43	50	4
Age		24 ± 1.7	40.6 ± 15.2	51.6 ± 18.2	56.2 ± 15.0	-
Gender	**Male**	4	23	22	26	-
	Female	4	24	21	24	-
Severity	**Severe**	–	0	–	–	–
	Nonsevere		47			
Days after symptom onset		–	26.8 ± 7.8	–	–	–
Source		Shanghai Jiao Tong University, Shanghai	Foshan 4th Hospital, Guangdong	Tongren Hospital, Shanghai	Tongren Hospital, Shanghai Ruijin Hospital, Shanghai	Wuhan Institute of virology, Wuhan, China

2.3. RBD protein conjugated on magnetic beads

RBD protein was provided by Sanyou Biopharmaceuticals Co., Ltd. (Shanghai, China, Cat No. LZQ20200809). Briefly, a solution of 50 μL, 4 mg/mL EDC (Sigma−Aldrich, Missouri, USA, Cat No. E1769) and 100 μL, 4 mg/mL NHS (Thermo Fisher Scientific Inc., USA, Cat No. 24500) were added to a 2 mL reaction tube mixed with 50 μL, 1 mg beads to activate beads at 25 °C for 30 min. All components were dissolved or suspended in MEST (50 mM, pH = 6.0). After washing the beads with MEST once, 200 μL of 0.03 mg/mL RBD solution was mixed with the beads immediately and incubated for 2 h. The supernatant was removed by magnetic adsorption, and the beads were washed 3 times with blocking buffer (containing PBS with 0.5% BSA and 0.3% glycine). Finally, the RBD beads were blocked with 400 μL blocking buffer (containing PBST with 0.1% BSA and 0.03% Proclin 300 (Sigma−Aldrich, Missouri, USA, Cat No. 48914-U) overnight at 4 °C and stored at 4 °C until use.

2.4. Establishment of the UIM-COVID-19 assay

S2-78 peptides or RBD-coated beads were applied following a similar protocol. All procedures were performed using an HD-X Analyzer (Quanterix, Inc.). The beads were diluted in bead diluent to a concentration of 2.0×10^7 beads/mL. The detector antibodies biotinylated goat anti-human IgG and IgM (Sangon Biotech Co, Ltd, Shanghai, China, Cat No. D110152; D110159) were both diluted in detector diluent. For S2-78 peptide-coated beads, the detector antibodies were diluted to a concentration of 0.5 μg/mL. Streptavidin-β-galactosidase (SβG) concentrate was diluted to 50 pM in SβG diluent. For RBD-coated beads, the detector antibodies were diluted to 0.3 μg/mL, and the streptavidin-β-galactosidase (SβG) concentrate was diluted to 150 pM. The serum samples or SARS-CoV-2 standard neutralizing antibodies (National Institutes for Food and Drug Control, China, Cat No. 280034–202001) were diluted to the expected ratio using sample diluent. After inputting all reagents, the automated measuring procedure was accomplished by HD-X Analyzer. In the two-step assay, the reaction cuvette contained 25 μL of bead suspension, 100 μL of the sample, and 20 μL of the detector antibody and was incubated for 35.25 min for the first step. After washing 6 times with washing buffer, 100 μL SBG was added to the reaction cuvette and incubated for 5.25 min. In the three-step assay, the reaction cuvette was incubated for 15 min in the first step, which contained 25 μL of bead suspension and 100 μL of sample. The beads were washed to remove the residue, and 100 μL of detector antibodies was added for 5.25 min of incubation for the second step. The third step was the same as the second step. The beads were loaded onto the disc after washing and resuspending in RGP solution. The array disc was then sealed with oil and imaged with a high-resolution camera. After analysis of the images, the number of "1" and "0" wells was counted, and then the average number of enzyme-labeled protein molecules per bead (AEB) was calculated (Rissin et al., 2013). Four-parameter logistic regression was used to fit standard curves. All measurements were performed in duplicate. The limit of detection (LoD) was calculated by using the signal from the control group plus 3 times the standard deviation (SD).

2.5. Establishment of the flow cytometry assay

For comparison with the single-molecule array, flow cytometry was performed. These tests were performed on a BD Accuri C6 Flow Cytometer (BD, America). Briefly, 10 μL magnetic bead suspension including 2×10^4 beads, 100 serum samples (dilution ratio = 1:200) or SARS-CoV-2 standard neutralizing antibodies, 40 μL 0.1 mg/mL Cy5-conjugated goat-anti-human IgG (Sangon Biotech Co, Ltd, Shanghai, China, Cat No. D111118) or Cy5-conjugated goat-anti-human IgM (Biosynthesis Biotechnology Co., Ltd. Beijing, China, Cat No. bs-0345G-Cy5), and 50 μL Cas-PBST (10 mM, pH = 7.4, with a 1% mass concentration of casein sodium salt) were added to a 2 mL centrifuge tube and incubated for 1 h at 37 °C. After separation on a magnetic rack and washing 3 times with PBST, the beads were resuspended in 200 μL deionized water and tested by a BD Accuri C6 Flow Cytometer. A 40 μL mixture was used to calculate the mean value of fluorescence intensity.

2.6. Microarray-based serum analysis

Microarray-based serum analysis was completed as described previously (Jiang et al., 2020). Briefly, arrays containing proteins and peptides were blocked with 3% BSA-PBS buffer at room temperature (25 °C) for 3 h. After washing with PBST buffer (0.1% Tween 20 in PBS buffer) and drying, each slide was installed with a 16-chamber rubber gasket. Then, 200 μL of incubation buffer (serum diluted 1:200 with 1% BSA-PBST) was added to the subarray and incubated at room temperature (25 °C) for 12–16 h. The arrays were washed 3 times with PBST for 10 min each time. The arrays were incubated with diluted Cy3-conjugated goat anti-human IgG (Jackson ImmunoResearch Cat No. 109-165-008) and Alexa Fluor 647-conjugated donkey anti-human IgM (Jackson ImmunoResearch Cat No. 709-605-073) (1:1000) at room temperature (25 °C) for 1 h, washed 3 times with PBST, and dried by centrifugation. Finally, each slide was scanned using a LuxScan 10 K-A instrument (CapitalBio Corporation, Beijing, China) with 100% laser power and PMT 500. The signal intensity was extracted by GenePix Pro 6.0 software (Molecular Devices, CA, USA).

2.7. Enzyme-linked immunosorbent assay (ELISA)

SARS-CoV-2 RBD-specific IgG and IgM antibodies were measured using commercial kits from Vazyme Biotech Co., Ltd. (Nanjing, China, Cat No. DD3103, DD3111) according to the manufacturer's protocol. Briefly, 10 μL of serum sample and 100 μL of sample diluent were added to 96-well plates and incubated at 37 °C for 30 min. After washing 5 times with wash buffer, 100 μL of detection antibody was added and incubated at 37 °C for 30 min. After another 5 washes, tetramethylbenzidine substrate was added and incubated at 37 °C. After 10 min, the reaction was stopped with stopping buffer, and then the absorbance was measured at 450 nm using SpectraMax i3X (Molecular Devices, CA, USA).

2.8. Data analysis and visualization

Standard curves of each method were obtained as follows. For the single molecule array (Simoa), serial dilutions of serum were generated, beginning at a ratio of 1:200,000 and followed by 4 additional points of 5x dilution (except for the IgM test for S2-78, with a beginning ratio of 1:8000). The last point was obtained by testing the dilution buffer. For the traditional flow cytometry method, the dilution ratios were different, *i.e.*, 1:2,500, 1:5,000, 1:10,000, 1:25,000, and 1:50,000 for IgG and 1:1,000, 1:2,500, 1:5,000, 1:10,000, and 1:25,000 for IgM. After obtaining the AEB or fluorescence intensity, GraphPad Prism 8.0 was used to fit four-parameter logistic regression curves. Additionally, ROC curves were generated by different models, and the AUC value was also calculated by the inner algorithm. Box diagrams were used to show the range of AEB between different cohorts. *P* values were calculated using the Wilcoxon signed-rank test (two-sided). Asterisks indicate statistical significance. Forest plots were generated to indicate the range of AUC with 95% CIs. RStudio, GraphPad Prism 8.0 and Origin 2016 were used together to visualize these data.

3. Results

3.1. Establishment of an ultrasensitive immunoassay based on a digital approach for monitoring SARS-CoV-2-specific IgG and IgM responses

The schematic diagram and workflow are shown in Fig. 1. For bead functionalization, two types of beads were prepared, *i.e.*, RBD- and S2-

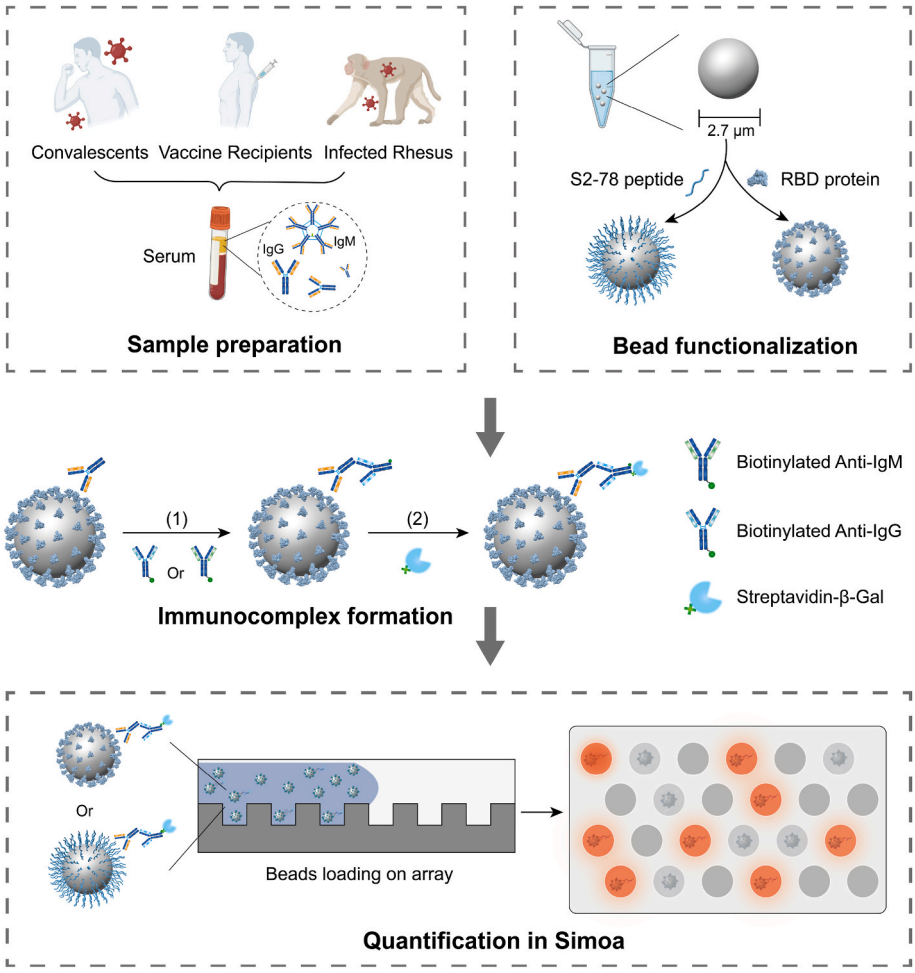

Fig. 1. Scheme of the ultrasensitive method to detect SARS-CoV-2-specific IgG and IgM antibodies. RBD: SARS-CoV-2 Spike protein Receptor Binding Domain, S2-78: A 12 amino acid peptide from Spike protein S2.

78 peptide-coated beads, while for sample preparation, three sets of samples were collected, *i.e.*, convalescents, inactivated virus vaccine-immunized donors and wild-type authentic SARS-CoV-2-infected rhesus monkeys (Table 1). Briefly, IgG and IgM antibodies were captured by excessive magnetic beads that were coated with RBD or S2-78 peptide. Based on *Poisson's distribution*, every single bead can capture one antibody at most (Rissin et al., 2013). After the formation of the immunocomplex (RBD/S2-78-coated beads + SARS-CoV-2 specific antibody + biotinylated detecting antibody (anti-IgM or anti-IgG) + streptavidin-β-galactosidase (SBG)), the suspension of the bead-based immunocomplex loaded into the microarray contained 216,000 microwells. The volume of each well is approximately 50 fL, which can accommodate only one bead. The substrate is catalyzed by an enzyme-linked immune complex on the surface of the beads to produce fluorescence; thus, by a high-resolution camera, the optical signal is transformed into digital signal "0" (representing no target in the microwell) or "1" (representing one target in the microwell). Counting the number of "1" and "0", the average number of enzymes per bead (AEB), corresponding to the average number of immunocomplexes per bead, was calculated (Rissin et al., 2013). With the help of a standard curve, ultrasensitive, accurate and digital quantification of pending samples is achieved.

To optimize the single-molecule assay, a convalescent serum sample was randomly chosen. We chose the signal-to-background ratio (SBR) as the index to determine the optimal conditions. For RBD-coated beads, the optimal concentration of the detecting antibody (Fig. S1A) and the optimal immobilized density of RBD onto the surface of the beads were set (Fig. S1B). For S2-78-coated beads, the optimal immobilized density of S2-78 for coating the beads (Fig. S1C) and the concentration of SBG (Fig. S1D) were also determined.

To reveal the limit of detection (LoD) of the established ultrasensitive immunoassay for monitoring SARS-CoV-2-specific IgG and IgM responses (UIM-COVID-19), RBD- and S2-78-coated beads were tested for both IgG and IgM (Fig. 2A-D). The convalescent serum sample used for optimization was serially diluted to set the calibration curves. As a comparison, a widely used flow cytometry detection method (Maia et al., 2020; O'Donnell et al., 2013) was also developed, optimized (Fig. S2) and performed on the same sample. The reasons for choosing the flow method are as follows: (1) Wider dynamic range (Rodrigues et al., 2017). (2) By using different magnetic beads and decoding methods, bead-based flow cytometry can be easily extended to detect multiple biomarkers simultaneously. (3) The same set of reagents (magnetic beads, capture antibody, detection antibody, etc.) could be used for both bead-based flow cytometry and Simoa, thus facilitating side-by-side comparison. As shown in Fig. 2, for RBD-IgG, the LoD of the single-molecule assay was 3 magnitudes higher than that of the flow cytometry assay (Fig. 2A and E), while for S2-78-IgG, the difference was an improvement of 2 magnitudes (Fig. 2B and F). For RBD-IgM and S2-78-IgM, the differences were both 2 magnitudes (Fig. 2C and G; Fig. 2D and H). When performing vertical comparison among the Simoa assays, it is clear that the sensitivity of RBD-coated beads is higher than that of S2-78-coated beads, and the IgG-based assay is more sensitive than the IgM-based assay (Fig. 2A-D).

We also used standard neutralizing antibodies to reveal the sensitivities of Simoa, flow cytometry assays and ELISA. The LoDs of the

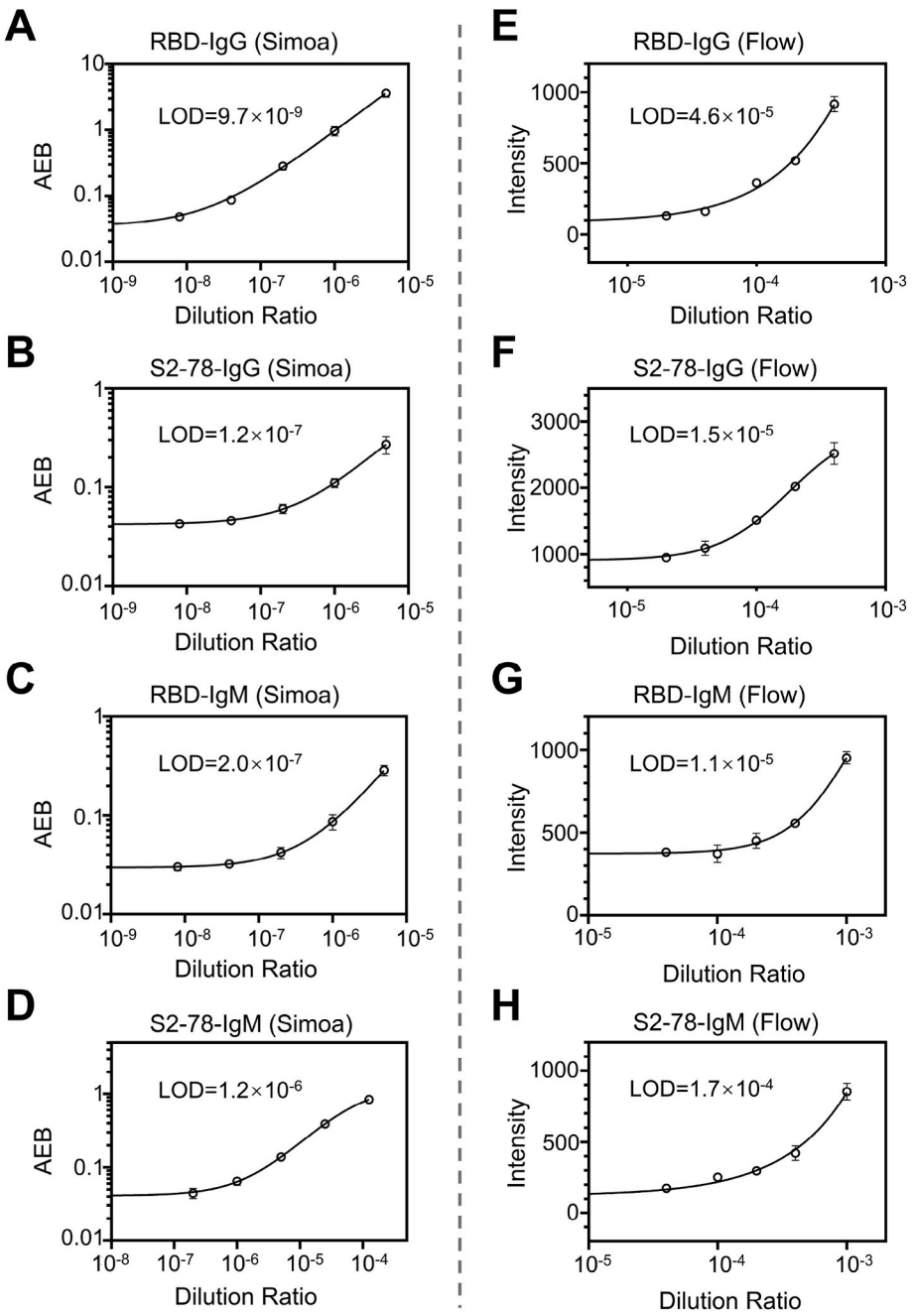

Fig. 2. Limit of detection (LOD) of Simoa- and flow cytometry-based immunoassays. A-D. Simoa assay. **A, B.** Standard curves of IgG detection using RBD (A)- and S2-78 (B)-coated beads. **C, D.** Standard curves of IgM detection using RBD (C)- and S2-78 (D)-coated beads. **E-H.** Flow cytometry assays. **E, F.** Standard curves of IgG detection using RBD (E)- and S2-78 (F)-coated beads. **G, H.** Standard curves of IgM detection using RBD (G)- and S2-78 (H)-coated beads.

single-molecule array were 5.2×10^{-6} and 1.1×10^{-5} U/mL for IgG (Fig. S3A) and IgM (Fig. S3B) detection, respectively, while the LoDs of the flow cytometry assay were 2.0×10^{-2} and 9.5×10^{-2} U/mL for IgG (Fig. S3C) and IgM (Fig. S3D), respectively, which is consistent with the results in Fig. 2. And the LoDs of ELISA are 1.16 and 0.41 U/mL for IgG (Fig. S3E) and IgM (Fig. S3F) detection, respectively.

To further validate the detection performance of the single-molecule assays, the precision of the UIM-COVID-19 assay was analyzed. Each concentration on the calibration curve was tested in duplicate, and each standard curve of the developed UIM-COVID-19 assay was generated from four replicates. The coefficient of variation (CV) was calculated from all measurements, and the CVs were <20% for most of the measurements, indicating good precision and reproducibility of both IgG and IgM detection (Figs. S4A and S4B).

In summary, we successfully established single-molecule assays for monitoring SARS-CoV-2-specific antibody responses, *i.e.*, UIM-COVID-19.

3.2. Significantly shorter seroconversion time windows were revealed by the single molecule assays for both IgG and IgM in comparison to that of flow cytometry assays

To determine the seroconversion times of SARS-CoV-2-specific antibody responses, 8 volunteers immunized with an inactivated virus vaccine (BBIBP CorV) were enrolled. Longitudinal sera were collected at 11 time points from these volunteers before vaccination until ~2 weeks after the 2nd dose of vaccine. These samples were then analyzed by the optimized UIM-COVID-19 assay and flow cytometry detection method

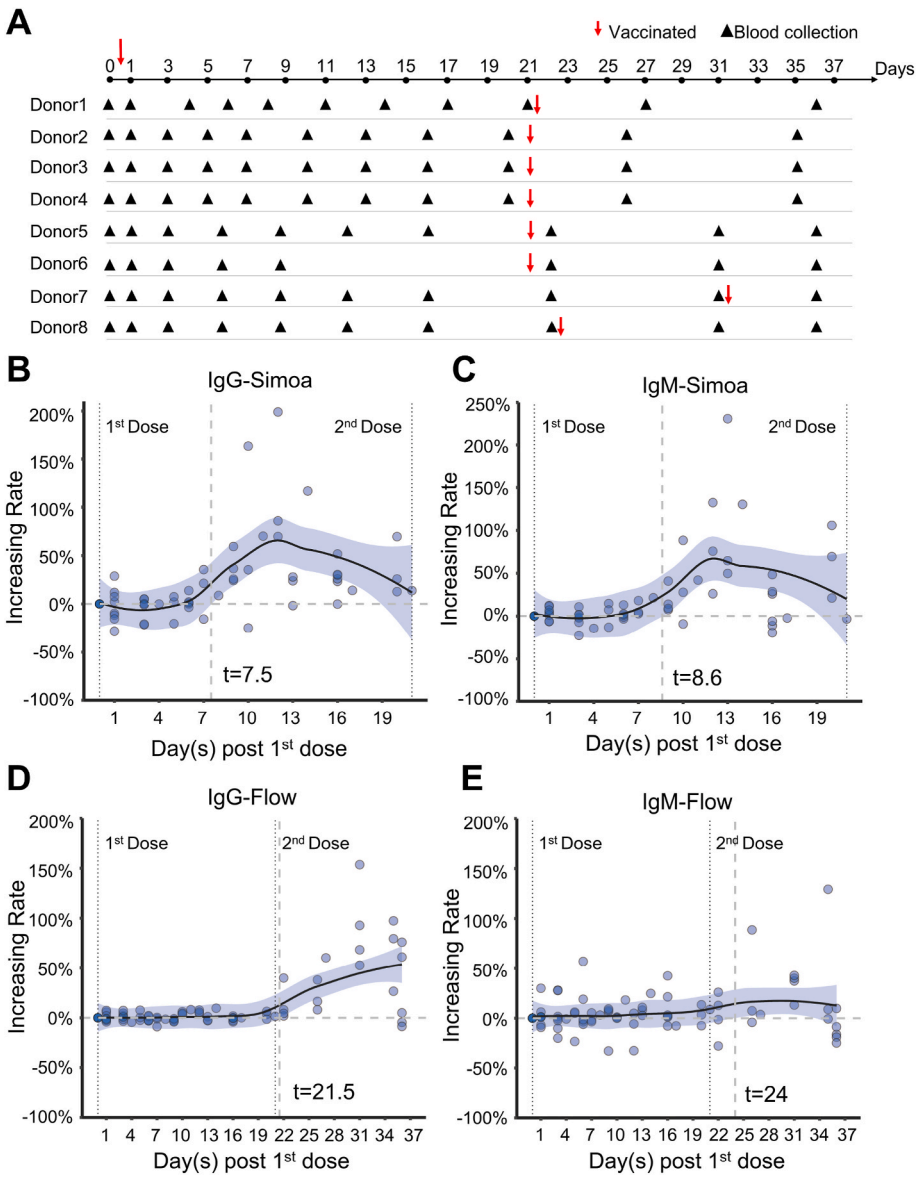

Fig. 3. Inactivated virus vaccine triggered IgG and IgM responses monitored by Simoa and flow cytometry assays. A. Longitudinal serum collection from eight donors (Donor1-Donor8). **B.** IgG response against RBD monitored by Simoa. **C.** IgG response against RBD monitored by flow cytometry. **D.** IgM response against RBD monitored by Simoa. **E.** IgM response against RBD monitored by flow cytometry. Locally weighted regression (LOESS) was applied to determine the earliest time point of seroconversion. The solid lines depict the median of the distribution, and the stripes around the regression line are equal-tailed 99% confidence intervals. The increasing rate was considered statistically significant if the equal-tailed 99% confidence interval of the posterior distribution did not overlap 0.

(Fig. 3A). The sera tested in these two assays were diluted at 1:200 to greatly reduce the interference of a large number of miscellaneous proteins in serum. To normalize the variation among individuals, locally weighted regression (LOESS) was used to imitate the increase in specific antibodies. To identify the earliest point when the vaccine-induced SARS-CoV-2-specific IgG or IgM antibodies begin to increase, the daily increasing rates (the day *vs*. the day before) were calculated and subjected to regression analysis. The increasing rate was considered statistically significant if the equal-tailed 99% confidence interval of the posterior distribution did not overlap 0.

Due to the high sensitivity of the UIM-COVID-19 assay, surprisingly, IgG evidently increased at 7.5 days after the first injection of vaccine (Fig. 3B), and IgM was also detected at almost the same time point, *i.e.*, 8.6 days (Fig. 3C). Meanwhile, by using flow cytometry to test the same set of samples, SARS-CoV-2-specific IgG and IgM could only be positively detected at 21.5 and 24 days after the 1st dose of vaccine, respectively (Fig. 3D and E). Notably, these time points of seroconversion determined by flow cytometry are later than the 2nd dose of vaccination (~21 days after the 1st dose mostly). It is possible that traditional methods, such as flow cytometry, could not detect the weak IgG response triggered only by the 1st dose of vaccine, which is consistent with Denis and Serap et al. (Sauré et al., 2022; tekol, 2021). These results were also verified by a protein microarray method (Jiang et al., 2020) and commercial ELISA kits, which showed almost the same detection time point as that of the flow cytometry assay (Fig. S5). The results of individual volunteers are shown in Fig. S6. Significantly increased antibody responses were observed in the UIM-COVID-19 assay for both IgG and IgM. Furthermore, the IgG and IgM antibodies were also tested with S2-78-coated beads, and no seroconversion was observed for IgG and IgM (Fig. S7). This indicates that the sensitivity of S2-78 is lower than that of RBD, which is consistent with previous studies (Li et al., 2021b).

In summary, we explored the seroconversion times of SARS-CoV-2-specific antibody responses after vaccination with the inactivated virus vaccine. Our data clearly demonstrated that by using the UIM-COVID-19 assay we developed here, the seroconversion times for both IgG and IgM just after the 1st vaccination were ~2 weeks earlier than those determined by the traditional assay (flow cytometry).

3.3. S2-78-based single molecule assays are suitable for COVID-19 diagnostics

To evaluate whether the S2-78 peptide can distinguish convalescents from healthy people and other patients with various diseases, the SARS-CoV-2-specific IgG response was measured by the UIM-COVID-19 assay using S2-78 and RBD as probes (Fig. 4A and B). Also, the flow cytometry assay was used for comparison (Fig. 4C and D). The sera for the UIM-COVID-19 assay were diluted at 1:10,000, while for flow cytometry, the dilution was 1:200. These dilutions were set to assure the best performance of each method. Receiver operating characteristic (ROC) curves of IgG and IgM in all models are shown in Fig. S8. Forest plots were applied to show the AUC values of different models (Fig. 4E and F). From the IgG response, the AUC of the RBD probe using the UIM-COVID-19 assay was as high as 1 (1-1, 95% CI) when compared to healthy people or patients with other diseases, suggesting that it can perfectly distinguish between uninfected people and COVID-19 patients. Meanwhile, the AUC of the S2-78 peptide was also high, *i.e.*, 0.983 (0.964–1, 95% CI) in distinguishing COVID-19 from healthy people and 0.897 (0.833–0.961, 95% CI) from other diseases (Fig. 4E). However, in regard to the flow cytometry assay, the AUC values of the RBD group were almost unaffected, while those of the S2-78 peptide group dropped significantly.

In addition, when employing IgM for detection, the trends were similar to those of IgG. However, as IgM antibodies appear at the early stage of infection, IgM from convalescent serum may decrease to an extremely low degree or may be eliminated by the immune system (Long et al., 2020; Lou et al., 2020; Noda et al., 2021). Hence, it is not accurate enough to perform IgM-based detection by traditional assays, such as ELISA. Fortunately, our ultrasensitive UIM-COVID-19 digital assay still has fairly good performance, with AUCs of 0.962 (0.918–1, 95% CI) and 0.940 (0.896–0.983, 95% CI) between COVID-19 convalescents and healthy people for RBD and S2-78 peptide, respectively (Fig. 4F).

These results suggest that by combining the ultrasensitive single

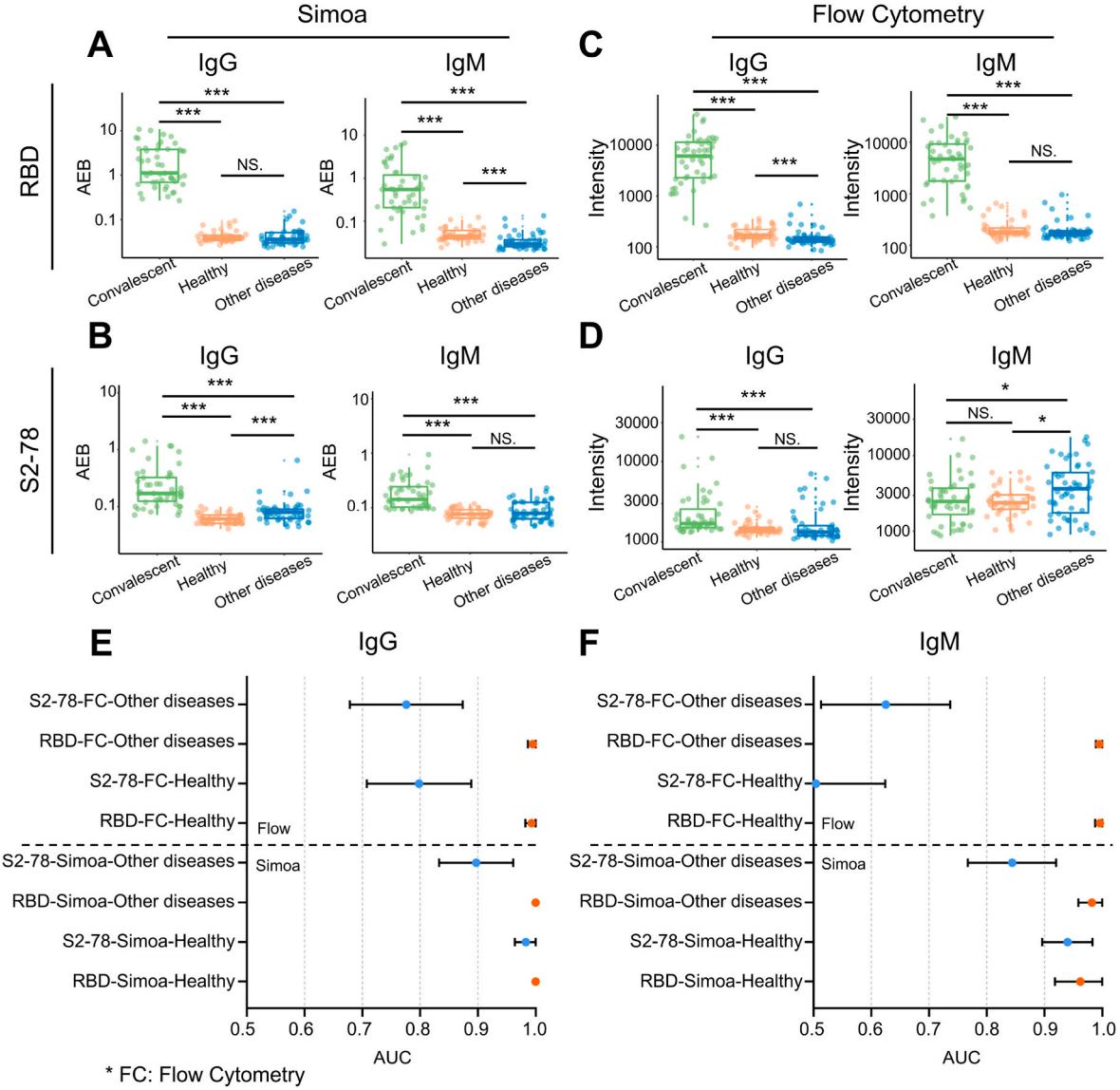

Fig. 4. IgG and IgM responses for COVID-19 diagnosis. Three groups of samples were included, *i.e.*, convalescent patients (n = 47), healthy group (n = 43), and patients with other diseases (n = 50). A. Box diagram of IgG and IgM for distinguishing different sample groups by Simoa using RBD-coated beads. **B.** Box diagram of IgG and IgM for distinguishing different sample groups by flow cytometry assays using RBD-coated beads. **C.** Box diagram of IgG and IgM for distinguishing different sample groups by Simoa using S2-78-coated beads. **D.** Box diagram of IgG and IgM for distinguishing different sample groups by flow cytometry assays using S2-78-coated beads. P values were calculated using the Wilcoxon signed-rank test (two-sided). Asterisks indicate statistical significance. P value: NS, >0.05; *, <0.05; **, <0.01; ***, <0.001. **E, and F.** Forest plots show the area under the curve (AUC) with 95% CIs for each assay.

molecule assay, the S2-78 peptide has the potential to be applied for highly sensitive COVID-19 diagnostics in clinical practice.

4. Discussion

The time window of seroconversion after viral infection is of great clinical significance and determines the earliest time point of clinical diagnosis and intervention. It is well known that upon viral infection, *e.g.*, SARS-CoV-2 infection, the seroconversion times for IgG and IgM are at least approximately 2 weeks and 1 week (Long et al., 2020; Lou et al., 2020), respectively. This concept was established based on traditional assays, such as ELISA. However, because of the limited sensitivity of the traditional assays, the known seroconversion times may not be absolute accurate. To address this, we took advantage of the high specificity of the RBD and the single-molecule sensitivity of the Simoa platform and established an ultrasensitive immunoassay for monitoring SARS-CoV-2-specific IgG and IgM responses, *i.e.*, UIM-COVID-19.

By using the traditional flow cytometry assay as the control, it is clear that the seroconversion times determined by the UIM-COVID-19 assay are ~2 weeks earlier for both IgG and IgM after injection of the 1st dose of the inactivated vaccine vaccination. By flow cytometry, the seroconversion times of IgG and IgM are both approximately 3 weeks, which are longer than what we already know. This could be explained by the lower antibody responses triggered by the 1st dose of the inactivated virus vaccine than that of the real-world infection (Ma et al., 2021). In addition, the same set of sera was also analyzed on the SARS-CoV-2 proteome microarray and ELISA kits. According to the RBD signal, the seroconversion times of IgG and IgM were 24.4 and 22.6 days, respectively. For ELISA, the seroconversion times of IgG and IgM were 21.6 and 20.7 days, respectively, which are similar to those of flow cytometry. The microarray and ELISA data could also serve as controls to further support the earlier seroconversion times determined by the UIM-COVID-19 assay. Furthermore, this was also confirmed by analyzing sera collected from rhesus monkeys challenged with the authentic SARS-CoV-2 virus, which showed 6.6 days of seroconversion (Fig. S9). It is anticipated that the antibody responses for a COVID-19 patient triggered by the real infection could be stronger; thus, it is possible that the seroconversion times could be further shortened.

Partially because of the lower sensitivity of traditional immunoassays for COVID-19 diagnosis, immunoassays are usually applied only as a second choice after NAT. As demonstrated in this study, much higher sensitivity and much shorter seroconversion windows were achieved by the UIM-COVID-19 assay. When this ultrasensitive assay is further validated in a larger cohort of independent samples, it has a much greater probability of being applied as an alternative, not just complementary, approach for the early diagnosis of COVID-19.

As mentioned above, before this study, the common knowledge is that the virus-triggered seroconversion times for IgG and IgM, including SARS-CoV-2 and other viruses, are ~2 weeks and ~1 week, respectively. Conceptually, our results demonstrated that the antibody seroconversion times are not fixed but limited to the sensitivity of the assay. When an approach of higher sensitivity is applied, a shorter seroconversion window can be confidently determined. Except for the single-molecule Simoa platform that we used to study COVID-19, it is no doubt that other high-sensitivity platforms could also be applied to the study of other viral infections, thus revealing more detailed information on virus-specific antibody responses at early stages. In turn, this information in general could strengthen our understanding of viral infection and provide important guidance for the prevention, detection and treatment of viral infections.

Another aim of this study was to explore the possibility of combining a peptide (S2-78) and the Simoa platform for the highly sensitive detection of COVID-19. The reasons for choosing peptide as probe are as follows: (1) Compared with S protein or RBD, the stability of peptide is much higher, thus, ease the preparation, storage, transportation, and delivery. (2) The cost of peptide is much lower. (3) This peptide contains only 12 amino acids and can be easily synthesized. When chemically synthesizing a large quantity of the peptide, the process could be well controlled, and high purity was assured. Thus, high reproducibility of the peptide-based assay could be achieved.

However, the peptide-based assay still has some limitations. Different from protein probes, small peptides have low molecular weights and poor accessibility on the surface of microspheres. Thus, by traditional ELISA or flow cytometry assays, it is difficult to achieve high performance. As a result, the peptide has not been widely used in clinical practice. However, with the help of the ultrasensitive Simoa platform, the S2-78 peptide demonstrated competitive capability in distinguishing COVID-19 convalescents from healthy people or patients with other diseases when compared to that of RBD.

Taken together, by taking advantage of the high sensitivity of single molecule-based technology, the high specificity of RBD, and the high reproducibility of the S2-78 peptide, we developed the UIM-COVID-19 assay to provide a new understanding of SARS-CoV-2-specific antibody responses from a unique perspective. The sensitivity of UIM-COVID-19 was 3846 and 8636 times higher than that of the flow assay for IgG and IgM, respectively (Figs. S3A–D). Compared with ELISA, UIM-COVID-19 was 2.2×10^5 and 3.7×10^4 times higher for IgG and IgM, respectively (Fig. S3 A-B, E-F). By applying this assay, a much shorter seroconversion window of IgG was determined, and the applicability of peptide S2-78 for COVID-19 diagnosis was also confirmed.

Early seroconversion detection of COVID-19 antibodies is vital. The potential clinical application is not limited to COVID-19 but also to many other diseases where shortening the detection window is of great significance, such as HIV. Obviously, due to the high cost, there is still some challenges to be overcome in how the current Simoa-based strategy can be widely used in ordinary clinical practice, and it may better serve as a platform of verification at this stage. Of course, how to combine ultrasensitive detection with point-of-care testing (POCT) to achieve a wide range of clinical applications is the direction that we are pursuing.

5. Conclusion

In this work, we combined the single molecule array platform (Simoa), RBD, and a previously identified SARS-CoV-2 S2 protein derivatized 12-aa peptide (S2-78) and developed an ultrasensitive assay (UIM-COVID-19 assay). Using longitudinal sera from 8 donors vaccinated with the inactivated virus vaccine, we found that the seroconversion time revealed by this assay was approximately two weeks earlier than that revealed by flow cytometry assays and conventional ELISA, which improves our understanding of the seroconversion time window after virus infection. In addition, by combining the ultrasensitive single molecule assay, the S2-78 peptide showed comparable diagnostic ability with the RBD protein, which means that the peptide has the potential to be applied for highly sensitive COVID-19 diagnostics in clinical practice. In summary, the single molecule-based SARS-CoV-2 assay is ultrasensitive and also paves a promising and powerful way for both immunological studies and diagnostics.

CRediT authorship contribution statement

Feiyang Ou: Investigation, Validation, Data curation, Visualization, Writing – original draft. **Danyun Lai:** Investigation, Validation, Data curation, Visualization, Writing – original draft. **Xiaojun Kuang:** Investigation. **Ping He:** Investigation. **Yang Li:** Investigation. **He-wei Jiang:** Investigation. **Wei Liu:** Investigation. **Hongping Wei:** Investigation. **Hongchen Gu:** Funding acquisition, Supervision. **Yuan qiao Ji:** Investigation. **Hong Xu:** Funding acquisition, Supervision, Writing – review & editing. **Sheng-ce Tao:** Funding acquisition, Supervision, Writing – review & editing.

Declaration of competing interest

The authors declare that they have no known competing financial interests or personal relationships that could have appeared to influence the work reported in this paper.

Data availability

Data will be made available on request.

Acknowledgments

This work was supported by the National Natural Science Foundation of China (Grant Nos. 21874091, 31927803, 31970130), the interdisciplinary program of Shanghai Jiao Tong University (YG2022ZD028), and Innovation Research Plan supported by Shanghai Municipal Education Commission (Grant No. ZXWF082101). We thank Tong Sun and Juanxi Gu of Shanghai Jiao Tong University for their data analysis assistance, and Jingwei Yi and Jiayu Zhang of Shanghai Jiao Tong University for their constructive discussion on graphics.

Appendix A. Supplementary data

Supplementary data to this article can be found online at https://doi.org/10.1016/j.bios.2022.114710.

References

Bosnjak, B., Stein, S.C., Willenzon, S., Cordes, A.K., Puppe, W., Bernhardt, G., Ravens, I., Ritter, C., Schultze-Florey, C.R., Godecke, N., Martens, J., Kleine-Weber, H., Hoffmann, M., Cossmann, A., Yilmaz, M., Pink, I., Hoeper, M.M., Behrens, G.M.N., Pohlmann, S., Blasczyk, R., Schulz, T.F., Forster, R., 2021. Cell. Mol. Immunol. 18 (4), 936–944.

Brouwer, P.J.M., Caniels, T.G., Straten, K.v.d., Snitselaar, J.L., Aldon, Y., Bangaru, S., Torres, J.L., Okba, N.M.A., Claireaux, M., Kerster, G., Bentlage, A.E.H., Haaren, M.M. v., Guerra, D., Burger, J.A., Schermer, E.E., Verheul, K.D., Velde, N.v.d., Kooi, A.v.d., Schooten, J.v., Breemen, M.J.v., Bijl, T.P.L., Sliepen, K., Aartse, A., Derking, R., Bontjer, I., Kootstra, N.A., Wiersinga, W.J., Vidarsson, G., Haagmans, B.L., Ward, A. B., Bree, G.J.d., Sanders, R.W., Gils, M.J.v., 2020. Science 369 (6504), 643–650.

Cai, Q.Y., Mu, J.J., Lei, Y., Ge, J., Aryee, A.A., Zhang, X.G., Li, Z.H., 2021. Anal. Bioanal. Chem. 413 (18), 4645–4654.

Dong, E., Du, H., Gardner, L., 2020. Lancet Infect. Dis. 20 (5), 533–534.

Gaylord, S.T., Abdul-Aziz, S., Walt, D.R., 2015. J. Clin. Microbiol. 53 (5), 1722–1724.

Gilboa, T., Cohen, L., Cheng, C.A., Lazarovits, R., Uwamanzu-Nna, A., Han, I., Griswold, K., Barry, N., Thompson, D.B., Kohman, R.E., Woolley, A.E., Karlson, E.W., Walt, D., 2021. Angew. Chem. Int. Ed. 60 (49), 25966–25972.

Jiang, H.W., Li, Y., Zhang, H.N., Wang, W., Yang, X., Qi, H., Li, H., Men, D., Zhou, J., Tao, S.C., 2020. Nat. Commun. 11 (1), 3581.

Killingley, B., Mann, A.J., Kalinova, M., Boyers, A., Goonawardane, N., Zhou, J., Lindsell, K., Hare, S.S., Brown, J., Frise, R., Smith, E., Hopkins, C., Noulin, N., Londt, B., Wilkinson, T., Harden, S., McShane, H., Baillet, M., Gilbert, A., Jacobs, M., Charman, C., Mande, P., Nguyen-Van-Tam, J.S., Semple, M.G., Read, R.C., Ferguson, N.M., Openshaw, P.J., Rapeport, G., Barclay, W.S., Catchpole, A.P., Chiu, C., 2022. Nat. Med.

Lee, C.Y., Lin, R.T.P., Renia, L., Ng, L.F.P., 2020. Front. Immunol. 11, 879.

Li, Y., Lai, D.Y., Lei, Q., Xu, Z.W., Wang, F., Hou, H., Chen, L., Wu, J., Ren, Y., Ma, M.L., Zhang, B., Chen, H., Yu, C., Xue, J.B., Zheng, Y.X., Wang, X.N., Jiang, H.W., Zhang, H.N., Qi, H., Guo, S.J., Zhang, Y., Lin, X., Yao, Z., Pang, P., Shi, D., Wang, W., Yang, X., Zhou, J., Sheng, H., Sun, Z., Shan, H., Fan, X., Tao, S.C., 2021a. Cell. Mol. Immunol. 18 (3), 621–631.

Li, Y., Ma, M.L., Lei, Q., Wang, F., Hong, W., Lai, D.Y., Hou, H., Xu, Z.W., Zhang, B., Chen, H., Yu, C., Xue, J.B., Zheng, Y.X., Wang, X.N., Jiang, H.W., Zhang, H.N., Qi, H., Guo, S.J., Zhang, Y., Lin, X., Yao, Z., Wu, J., Sheng, H., Zhang, Y., Wei, H., Sun, Z., Fan, X., Tao, S.C., 2021b. Cell Rep. 34 (13), 108915.

Long, Q.X., Liu, B.Z., Deng, H.J., Wu, G.C., Deng, K., Chen, Y.K., Liao, P., Qiu, J.F., Lin, Y., Cai, X.F., Wang, D.Q., Hu, Y., Ren, J.H., Tang, N., Xu, Y.Y., Yu, L.H., Mo, Z., Gong, F., Zhang, X.L., Tian, W.G., Hu, L., Zhang, X.X., Xiang, J.L., Du, H.X., Liu, H. W., Lang, C.H., Luo, X.H., Wu, S.B., Cui, X.P., Zhou, Z., Zhu, M.M., Wang, J., Xue, C. J., Li, X.F., Wang, L., Li, Z.J., Wang, K., Niu, C.C., Yang, Q.J., Tang, X.J., Zhang, Y., Liu, X.M., Li, J.J., Zhang, D.C., Zhang, F., Liu, P., Yuan, J., Li, Q., Hu, J.L., Chen, J., Huang, A.L., 2020. Nat. Med. 26 (6), 845–848.

Lou, B., Li, T.D., Zheng, S.F., Su, Y.Y., Li, Z.Y., Liu, W., Yu, F., Ge, S.X., Zou, Q.D., Yuan, Q., Lin, S., Hong, C.M., Yao, X.Y., Zhang, X.J., Wu, D.H., Zhou, G.L., Hou, W. H., Li, T.T., Zhang, Y.L., Zhang, S.Y., Fan, J., Zhang, J., Xia, N.S., Chen, Y., 2020. Eur. Respir. J. 56 (2).

Ma, M.L., Shi, D.W., Li, Y., Hong, W., Lai, D.Y., Xue, J.B., Jiang, H.W., Zhang, H.N., Qi, H., Meng, Q.F., Guo, S.J., Xia, D.J., Hu, J.J., Liu, S., Li, H.Y., Zhou, J., Wang, W., Yang, X., Fan, X.L., Lei, Q., Chen, W.J., Li, C.S., Yang, X.M., Xu, S.H., Wei, H.P., Tao, S.C., 2021. Cell Discov 7 (1), 67.

Maia, J., Batista, S., Couto, N., Gregorio, A.C., Bodo, C., Elzanowska, J., Strano Moraes, M.C., Costa-Silva, B., 2020. Front. Cell Dev. Biol. 8, 593750.

Noda, K., Matsuda, K., Yagishita, S., Maeda, K., Akiyama, Y., Terada-Hirashima, J., Matsushita, H., Iwata, S., Yamashita, K., Atarashi, Y., Watanabe, S., Ide, N., Yoshida, T., Ohmagari, N., Mitsuya, H., Hamada, A., 2021. Sci. Rep. 11 (1), 5198.

Norman, M., Gilboa, T., Ogata, A.F., Maley, A.M., Cohen, L., Busch, E.L., Lazarovits, R., Mao, C.P., Cai, Y., Zhang, J., Feldman, J.E., Hauser, B.M., Caradonna, T.M., Chen, B., Schmidt, A.G., Alter, G., Charles, R.C., Ryan, E.T., Walt, D.R., 2020. Nat Biomed Eng 4 (12), 1180–1187.

O'Donnell, E.A., Ernst, D.N., Hingorani, R., 2013. Immune Netw 13 (2), 43–54.

Ogata, A.F., Cheng, C.A., Desjardins, M., Senussi, Y., Sherman, A.C., Powell, M., Novack, L., Von, S., Li, X., Baden, L.R., Walt, D.R., 2021. Clin. Infect. Dis.

Preische, O., Schultz, S.A., Ape, A., 2019. Nat. Med.

Rissin, D.M., Wilson, D.H., Duffy, D.C., 2013. Measurement of Single Protein Molecules Using Digital ELISA, the Immunoassay Handbook, pp. 223–242.

Rodrigues, V., Baudier, J.B., Chantal, I., 2017. Cytometry 91 (9), 901–907.

Ryan, K.A., Bewley, K.R., Fotheringham, S.A., Slack, G.S., Brown, P., Hall, Y., Wand, N.I., Marriott, A.C., Cavell, B.E., Tree, J.A., Allen, L., Aram, M.J., Bean, T.J., Brunt, E., Buttigieg, K.R., Carter, D.P., Cobb, R., Coombes, N.S., Findlay-Wilson, S.J., Godwin, K.J., Gooch, K.E., Gouriet, J., Halkerston, R., Harris, D.J., Hender, T.H., Humphries, H.E., Hunter, L., Ho, C.M.K., Kennard, C.L., Leung, S., Longet, S., Ngabo, D., Osman, K.L., Paterson, J., Penn, E.J., Pullan, S.T., Rayner, E., Skinner, O., Steeds, K., Taylor, I., Tipton, T., Thomas, S., Turner, C., Watson, R.J., Wiblin, N.R., Charlton, S., Hallis, B., Hiscox, J.A., Funnell, S., Dennis, M.J., Whittaker, C.J., Catton, M.G., Druce, J., Salguero, F.J., Carroll, M.W., 2021. Nat. Commun. 12 (1), 81.

Sauré, D., O'Ryan, M., Torres, J.P., Zuniga, M., Santelices, E., Basso, L.J., 2022. Lancet Infect. Dis. 22 (1), 56–63.

Shan, D., Johnson, J.M., Fernandes, S.C., Suib, H., Hwang, S., Wuelfing, D., Mendes, M., Holdridge, M., Burke, E.M., Beauregard, K., Zhang, Y., Cleary, M., Xu, S., Yao, X., Patel, P.P., Plavina, T., Wilson, D.H., Chang, L., Kaiser, K.M., Nattermann, J., Schmidt, S.V., Latz, E., Hrusovsky, K., Mattoon, D., Ball, A.J., 2021. Nat. Commun. 12 (1), 1931.

Speer, C., Goth, D., Benning, L., Buylaert, M., Schaier, M., Grenz, J., Nusshag, C., Kalble, F., Kreysing, M., Reichel, P., Tollner, M., Hidmark, A., Ponath, G., Schnitzler, P., Zeier, M., Susal, C., Morath, C., Klein, K., 2021. Clin. J. Am. Soc. Nephrol. 16 (7), 1073–1082.

tekol, s.d., 2021. Southern Clinics of Istanbul Eurasia.

Woo, P.C., Lau, S.K., Wong, B.H., Chan, K.H., Chu, C.M., Tsoi, H.W., Huang, Y., Peiris, J. S., Yuen, K.Y., 2004. Clin. Diagn. Lab. Immunol. 11 (4), 665–668.

Xie, C., Ding, H., Ding, J., Xue, Y., Lu, S., Lv, H., 2022. J. Med. Virol. 94 (4), 1633–1640.

Xue, J.B., Lai, D.Y., Jiang, H.W., Qi, H., Guo, S.J., Zhu, Y.S., Xu, H., Zhou, J., Tao, S.C., 2022. Cell Discov 8 (1), 15.